

SCIENTIFIC REPORTS



OPEN

Knockdown of a cellulose synthase gene *BoiCesA* affects the leaf anatomy, cellulose content and salt tolerance in broccoli

Received: 25 August 2016
Accepted: 19 December 2016
Published: 07 February 2017

Shuangtao Li^{1,*}, Lei Zhang^{1,*}, Ying Wang^{1,2,*}, Fengfeng Xu^{1,*}, Mengyun Liu¹, Peng Lin¹, Shuxin Ren³, Rui Ma⁴ & Yang-Dong Guo¹

Cellulose is the major component of cell wall materials. A 300 bp specific fragment from the cDNA fragment was chosen to insert into vector pFGC1008 at forward and reverse orientations to construct the recombinant RNAi vector. Knockdown of *BoiCesA* caused "dwarf" phenotype with smaller leaves and a loss of the content of cellulose. Moreover, RT-PCR analysis confirmed that the expression of the RNAi apparatus could repress expression of the *CesA* gene. Meanwhile, examination of the leaves from the T3 of RNAi transformants indicated reduction of cell expansion in vascular bundles, particularly on their abaxial surface. The proline and soluble sugar content increased contrarily. Under the salt stress, the T3 of RNAi plants showed significant higher resistance. The expression levels of some salt tolerance related genes (*BoiProH*, *BoiPIP2;2*, *BoiPIP2;3*) were significantly changed in T3 of RNAi plants. The results showed that the hairpin structure of *CesA* specific fragment inhibited the endogenous gene expression and it was proved that the cDNA fragment was relevant to the cellulose biosynthesis. Moreover, modulation cellulose synthesis probably was an important influencing factor in polysaccharide metabolism and adaptations of plants to stresses. This will provide technological possibilities for the further study of modulation of the cellulose content of crops.

Dietary fiber is believed to protect against a series of diseases¹. Most of dietary fiber is from cell walls of plants. Cellulose, an essential component of both primary and secondary cell walls of high plants², is composed of (1 → 4)-β-D-glucan chains³. The first plants cellulose synthase (*CesA*) gene was cloned in 1996⁴ and the isolation of cellulose synthase complex was difficult⁵. The discovery of acotton gene suspected to encode *CesA* brought the field of plant cell wall biogenesis into the genomic era⁶. Many *CesA* and *CesA*-like (*Csl*) genes have been isolated in plants by far^{7–10}.

Sequence analyses of the *CesA* genes indicated that they encoded family II glycosyl transferases^{11,12}. These enzymes contained two domains designated A and B. Domain A contained the D...D motif common to all family II glycosyltransferases while domain B carried an additional conserved D residue as well as the QxxRW motif^{11–13}. Structural evidence of family II and other glycosyl transferases suggested that the A domain binded the nucleotide sugar and the B domain binded the acceptor substrate, together forming a viable catalytic center^{14,15}. Moreover, there were two N-terminal putative zinc finger domains in the *CesA* proteins, and might play a key role in the dimerization of the *CesA* catalytic subunits and the rosette assembly¹⁶. A series of mutants can be used to analysis the function of different *CesA* genes. For example, temperature-sensitive *root-tip swelling* mutant (*rsw1*) of *Arabidopsis* showed a decline of cell wall cellulose content and a dwarf phenotype¹⁷. The defective *AtCesA6* mutant (*prc1*) presented dwarf-hypocotyl¹⁸. The *irx1* and *irx3* mutant, displaying a phenotype of collapsed mature xylem cells and reduced content of secondary cell wall cellulose, were determined to be *CesA* homologues^{19–21}. Moreover, the expression levels of *CesA* RNA and accumulation of cellulose content have been evaluated in tobacco²².

¹College of Horticulture, China Agricultural University, 100193, Beijing, China. ²Horticulture Research Institute, Shanghai Academy Agricultural Sciences, Shanghai 201403, China. ³School of Agriculture, Virginia State University, PO Box 9061, Petersburg, VA23806, USA. ⁴Agro-Biotechnology Research Institute, Jilin Academy of Agricultural Sciences, Changchun 130033, China. *These authors contributed equally to this work. Correspondence and requests for materials should be addressed to Y.-D.G. (email: yaguo@cau.edu.cn)

By antisense expression of different potato *CesA* clones, the cellulose content of tuber cell walls dropped to 40% of the control plant and the recombinant constructs are efficient to control the cellulose synthesis²³. Currently, we focused on using RNAi to changes cellulose levels and anatomic characteristics of broccoli. The correlation of anatomic changes and plant physiological character was also discussed. The aim of present study is mainly regulate the content of cellulose, so as to improve the quality of vegetables.

Materials and Method

Amplification of the broccoli *CesA* fragment. Total RNA was extracted from young leaves of broccoli by using the procedure of phenol-guanidine isothiocyanate (Trizol, invitrogen). The RNA was then used as template to synthesize the cDNA.

We used the following sequences: cotton *GhCesA* (U28583 and U28584⁴), *ArabidopsisAtCesA1* (AAC39334.1¹⁷), *AcetobacterBcsA* (M37202), *AcetobacterAcsA* (X54676) as described in ref. 24, primers were designed according to the *CesA* genes in cotton, *Arabidopsis*, *Acetobacter xylinum*. Fragments of cDNAs from broccoli, designated *CesA-a*, *CesA-b*, *CesA-c*, *CesA-d*, *CesA-e* were amplified by PCR from 1 μ L of the cDNA reaction mixture with primer combinations, as follows: *CesA-a*, 5' primer 5'-CTCATCTATGTTTCTCGTGA-3' and 3' primer 5'-GCATCTTGAACCCAGTAA-3'; *CesA-b*, 5' primer 5'-TAACAGGGA-GACTTATCTTGACCG-3' and 3' primer 5'-GGAACTGGACATAGCACACTT-3'; *CesA-c*, 5' primer 5'-GGAAAGATGGAACTCAGTG-3' and 3' primer 5'-CGTTACAAGAGGAG-GCTC-3'; *CesA-d*, 5' primer 5'-CGTGTGAAGATGGAGA-3' and 3' primer 5'-AGATTG-TGTATCAGGCGTGC-3'; *CesA-e*, 5' primer 5'-AGTGTAAAGAAAGCGTTTGGTCA-3' and 3' primer 5'-CAATGACCCAGAAGTCTCG-3'. PCR amplification was performed with standard PCR buffer, 50 ng of both *CesA* primers, and 2.5 units of Taq polymerase (TAKARA-A). The BLAST programs, Clustal analysis and multiple alignment of the DNAMAN program package, were used to analyze the homology of cDNA sequences.

Total RNA was extracted from various tissues of four-week-old wild type plants. Quantitative real-time PCR was carried out in ABI7500 system with the SYBR Premix Ex TaqTM kit (TAKARA, Japan). The primer pairs were used for the experiment as follows: *BoiCesA* primers, F (5'-CGTGTGAAGGAGATGGAGA-3'), R (5'-AGATTGTGTATCAGGCGT-GC-3'). *Actingene*(AF044573) primers, ActF (5'-TGGGATGAACCAGAAGGATGC-3') and ActR(5'-TGGC-GTAAAGGGAGAGGACA-3')30 cycles. The specific of primer pairs was checked (Fig. S1). Each experiment was replicated at least three times.

Construction of RNAi vector. A 300-bp class-specific region was amplified to construct the recombinant RNAi vector pFGCCesA which used the primers RiF containing *Bam*HI and *Spe*I sites (F1-AAAGGATCCAAAGATGGAACTCAGT; R1-GAAACTAGTGCACAGATTGTGTATCAG) and RiR containing *Asc*I and *Swa*I sites (F2-AAGGCGCGCCATTGTGTATCAGGC; R2-GGGATTTAAATGAGAGGAAAGATGG). The *BoiCesA* sense and antisense fragments were inserted into pFGC1008 to construct the recombinant vector. The selection of specific cDNA fragment referred to the method that used virus-induced gene silencing which published in the Plant Cell²⁵. The vector was transferred into *Agrobacterium tumefaciens* strain EHA105 by the freeze-thaw method²⁶.

Genetic transformation of broccoli. The broccoli variety 05-33-105 was used for transformation. It was implemented with *Agrobacterium tumefaciens* strain EHA105 harboring pFGCCesA constructs and using plasmid pFGC1008 as control. The recombinant plasmid includes the *HPTII* coding region which was used as a selectable marker (conferring hygromycin resistance).

A hygromycin sensitivity test was performed using cotyledon and hypocotyl explants from seven-day-old seedling²⁷. Hypocotyl and cotyledon explants were pre-incubated on the shoot induction medium (MS medium containing 2 mg/L ZT and 0.01 mg/L IAA) for two days in darkness. The incubated explants were immersed into the *Agrobacterium tumefaciens* solution for 4–8 min (to the hypocotyls and cotyledons) with gentle shaking. The explants were then transferred on the co-cultivation media (MS medium containing 2 mg/L ZT, 0.01 mg/L IAA and 100 μ M AS). After co-cultivation for two days in darkness, the explants were transferred to the same basal medium which was supplemented with 350 mg/L carbenicillin and cultured for seven days. Then the explants were transferred on the selection medium which was supplemented with hygromycin at 4 mg/L and carbenicillin at 200 mg/L for another 4–6 weeks to induce shoots. When the shoots emerged, they were subjected to transfer to another medium (MS medium containing 0.5 mg/L NAA and 5 mg/L hygromycin) for root induction. Finally the regenerated plants were transferred to soil. After being vernalized, the seeds of progeny were obtained. The transgenic lines (T3 lines) were used for further experiments.

Southern blotting. The genomic DNA was extracted from control and transgenic plants, using *Bam*HI to digest the DNA. The DNA was transferred and cross-linked onto a nylon membrane. The selectable hygromycin phosphotransferase gene (*HPTII*) was labeled by PCR for hybridization (Dig Easy Hyb). Then the membrane was washed with different concentration of SSC. At last the membrane was exposed to X-ray²⁸. The primers of *HPTII* gene is 5'-CGTGTGAAGGAGAT-GGAGA-3' and 5'-AGATTGTGTATCAGGCGTGC-3'.

Microscopy analysis. For light microscopy, developed leaves were used to prepare sections by microtome and it were stained with safranin-fast green, then observed and photographed under a light microscope²⁹. For scanning electron microscopy (SEM), the methods are detailed by Yu *et al.*³⁰. Small leaf tissues were fixed with 2.5% buffered glutaraldehyde. Then, it was transferred to 1% osmium tetroxide fixative and dehydrated in an ethyl alcohol series from 30 to 100%. The important step was critical point dried and gold coated transmission electron microscopy (TEM) sampling and preparation were carried out as described in the standard procedure³¹.

Measurement of carbohydrate. Cell walls were prepared based on previous methods^{32,33}. Briefly, using the phenol-methanol to eliminate lipid and protein from the sample and extracting with ethanol and drying, the dried cell wall materials were used to analyze the cellulose content³⁴.

The measurement of pectin content was operated as described in papers^{35,36}. Shortly the sample powder with hot absolute ethanol was heated and then centrifuged at 10,000 rpm for 10 min. Alcohol insoluble solids (AIS) were obtained and the concentrated sulfuric acid was used to dissolve AIS. The mixture was transferred into a 25 ml volumetric flask. Then sample solution was added to sodium tetraborate. Color development following addition of *m*-hydroxydiphenyl, the galacturonic acid was gained that was equal to total pectin content.

Reverse Transcription PCR method. Leaves were picked from T3 of RNAi plants and ground to the fine powder in liquid nitrogen, total RNA was extracted according to the method described by the scription of Trizol. Ten µg of RNA was used for cDNA synthesis with oligo (DT)₁₈ as the primer and 1 µL of cDNA was applied in the PCR reaction. The cycle numbers and transcript levels were optimized.

Proline and soluble sugar content determination. Two independent transgenic lines were selected to measure the proline and soluble sugar content. The measurement of proline content in leaves was prepared according to the method reported by Troll and Lindsley³⁷. The content of soluble sugar was then measured³⁸.

Evaluation of NaCl to tolerance for T3 of RNAi plants. The control plants and RNAi plants were kept in a chamber with normal growth condition as 16-h-light/8-h-dark cycle, 23 ± 1 °C, with 60% relative humidity. For NaCl treatments, the four-week-old potted plants were treated with 250 mM NaCl for 3 weeks.

The assay of antioxidant enzymes. Superoxide dismutase (SOD; EC 1.15.1.1) activity was measured based on its ability to inhibit the photochemical reduction of Nitroblue tetrazolium³⁹. Peroxidase (POD; EC 1.11.1.7) activity was measured at 25 °C by monitoring the increase in absorbance at 470 nm⁴⁰. Catalase (CAT; EC 1.11.1.6) activity was measured at 25 °C by the absorbance decrease at 240 nm due to the H₂O₂ decomposition⁴¹. Ascorbate peroxidase (APX; EC 1.11.1.11) activity was determined by monitoring the decrease in absorbance of ascorbic acid at 290 nm⁴².

Quantitative RT-PCR analysis of *BoiProDH*, *BoiPIP2;2* and *BoiPIP2;3*. The expressions of *BoiProDH*, *BoiPIP2;2* and *BoiPIP2;3* in WT and T3 of RNAi plants were analyzed by real-time quantitative reverse transcriptase using the fluorescent intercalating dye SYBRGreen in a detection system. The primer pairs were used for the experiment as follows: *BoiProDH* primers, F 5'-CAAGAAGCCGAGAAGAA-3', R 5'-CCAGAGTCAGCGTTATGT-3'. *BoiPIP2;2* primers, F 5'-TGTTTGGGTGCGATATGTGGAGTT-3', R 5'-GTGGCGGAGAAGACGGTGTAG-3'. *BoiPIP2;3* primers, F 5'-AAGGAAGGTATCGTTGGTTA-3', R 5'-AGTCTCGGGCATTCTTT-3'. Actin gene (AF044573) primers were same as mentioned above.

Statistical analysis. Statistical procedures were carried out with the software package SPSS11.0, Differences among treatments were analyzed taking $P < 0.05$ as significance according to Duncan's multiple range test. The relative estimate of the amount of cDNA in broccoli leaves was obtained by Image J software.

Results

Molecular cloning and comparative sequences analysis of *BoiCesA* cDNA. Five cDNA fragments from the *CesA* gene of broccoli were amplified by standard RT-PCR. Their positions based on the cell wall cellulose biosynthesis gene were shown (Fig. 1a)⁴, as described by Delmer⁵. The nucleotide sequences of cDNAs *CesA-a*, *CesA-b*, *CesA-c*, *CesA-d* and *CesA-e* were identical where they overlap each other. The cDNAs described the sequences of the same *CesA* gene. Based on the results of sequencing and assembly, a 3252 bp of the *CesA* cDNA fragment was identified from broccoli, its corresponding deduced amino acid contained D, D (aspartic acid residues) and QXXRW motif which was located at the catalytic site. The sequence of the cDNA was compared with the corresponding sequences of the *Populus tremuloides PtrCesA4* gene, *Acacia mangium AmCesA1* gene and the *Arabidopsis AtCesA1 (rsw1)* gene (Fig. 1b). Sequence analysis shows that the cDNA fragment designated *BoiCesA* is a member of *CesA* superfamily. It shared 90% identity with *AtCesA1* at the nucleotide level and 94% identity at the protein level.

Organ-specific expression of *BoiCesA* gene. To evaluate the transcript accumulation of *BoiCesA* gene in different organ, the results of quantitative real-time PCR revealed that *BoiCesA* was expressed in various organs of broccoli, including roots, stems and leaves (Fig. 2). Our results showed that the expression level of *BoiCesA* was the highest in leaf organs. There were significant differences ($P < 0.05$) in the expression level of *BoiCesA* between different organs.

Regulation of *CesA* gene expression in broccoli. A recombinant RNAi construct pFGCCesA was applied to regulate cellulose biosynthesis in broccoli (Fig. 3a). The 300 bp-length sense *BoiCesA* sequence and antisense *BoiCesA* sequence was amplified and inserted into pFGC1008 vector. The T-DNA region of pFGCCesA harbored the selectable hygromycin phosphotransferase gene (*HPTII*) for hygromycin resistance. Expression of the hairpin structure was driven by the constitutive CaMV 35S promoter.

The Southern blotting analysis for transgenic plants. The pFGC1008-*CesA* plasmid was transformed into broccoli and 65 plantlets from hypocotyls and 40 plantlets from cotyledons resistant to hygromycin were obtained. To further confirm that the phenotype of transgenic plants is due to the introduction of RNAi construct, southern blot was done in the control and transgenic plants (Fig. 3b). The wild type plants was used as control that is no band was detected. However, transgenic plants had different hybridization bands which were different size.

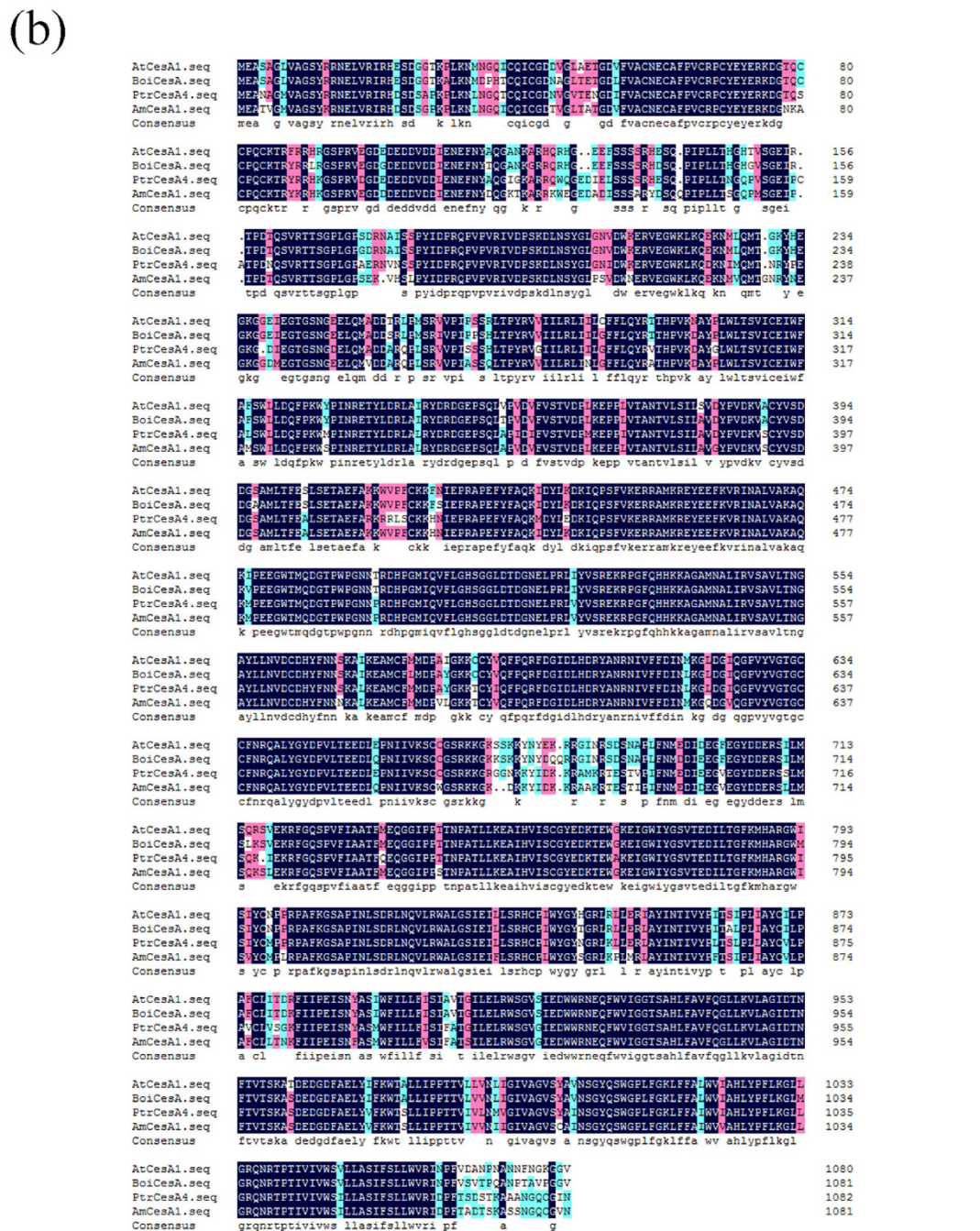
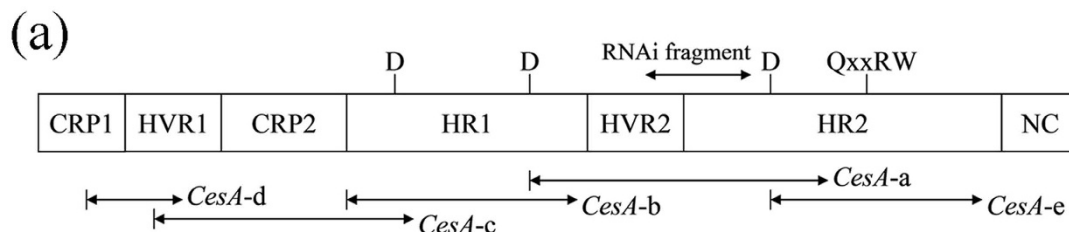


Figure 1. The construct of *BoiCesA* gene and the amino acid sequence alignments of the *Brassica oleracea* L. cellulose synthase *BoiCesA* with *CesA* genes of other plants. (a) Positions of the five cDNAs from broccoli were shown in relation to the regions of plant *CesA* genes. CRP: conserved plant-specific region; HVR: hypervariable plant-specific region; HR: homologous region of all *CesA* genes; NC: no obvious conservation; RNAi fragment: the target sequences of RNAi. (b) Amino acid sequence alignments of *BoiCesA* with the corresponding sequences of *CesA* from *Arabidopsis* (*AtCesA1*), *Populustremuloides* *PtrCesA4* and *Acacia mangium* *AmCesA1*.

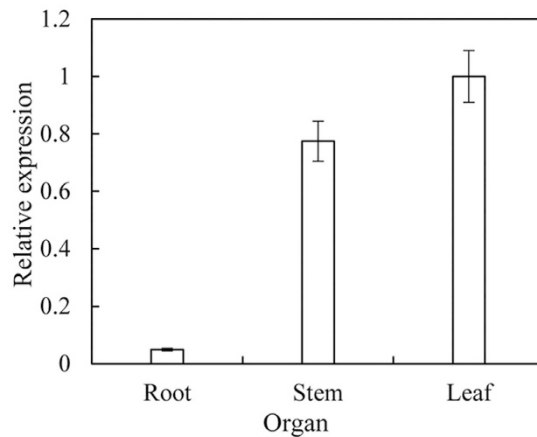


Figure 2. Detection of *BoiCesA* expression level in different organs of broccoli plants.

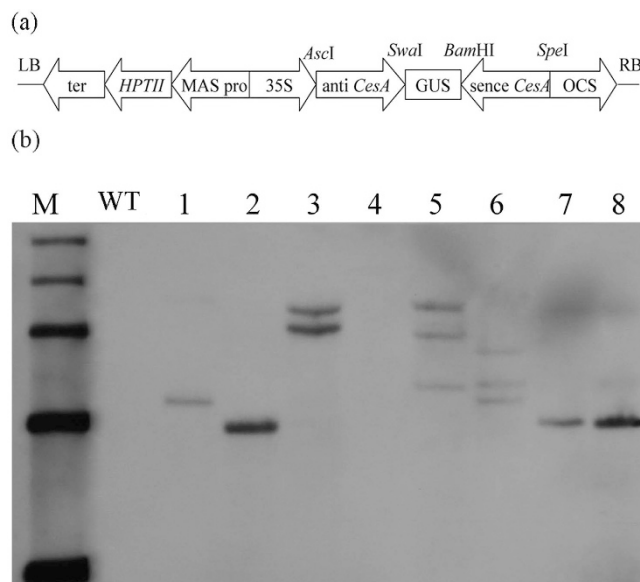


Figure 3. RNAi construct and Southern blotting detection of transgenic plants. (a) Schematic diagram of the RNAi construct named pFGCCesA. (b) Southern blotting detection of transgenic plants. M: Marker DL15000WT: wild-type plants 1–8: transgenic plants.

It suggested that the RNAi construct contained *BoiCesA* gene was random integrated into *Brassica oleracea*. We selected two independent RNAi lines RNAi-2 and RNAi-8 to do further research.

Transcriptional activity of the *CesA* gene in broccoli. In order to evaluate the effect of RNAi on *CesA* gene expression, RT-PCR experiments were performed to study these changed cellulose contents whether related to the expression of *BoiCesA* gene. The constitutive *Actin* gene⁴³ applied as the control in this study. It showed that the RT-PCR results with the *BoiCesA* and *Actin* primers in the transgenic plants and control plants (Fig. 4). The amplified product revealed that a reduction of the *BoiCesA* expression in the RNAi plants in relation to the control plants.

Phenotypes of the RNAi transformed plants. In order to observe the growth of control and knock-down plants, the germination performance of seeds was observed. There is no significant distinction between control and transgenic seeds (Fig. 5a). However transformed plants showed a typical dwarf phenotype (Fig. 5b) and had obvious change in plant height (Fig. 5c). Furthermore, it was evident to find that some surface lumps presented on the abaxial surfaces of the leaves, and the texture was crisp in the RNAi plants (Fig. 5d). The pFGC-CesA plants were shorter in stature than the control plants (transformed with pFGC1008) (Fig. 5e). Compared with the control plants, the RNAi plants had similar internode length but with less nodes (Fig. 5f). The leaves of the transgenic plants were smaller than those of the control plants, meanwhile the fresh weight decreased relative to that of control plants (Fig. 5g). These phenotypic characteristics had a good agreement with the corresponding observation in tobacco which had been silenced by a plant cellulose synthase gene²⁵.

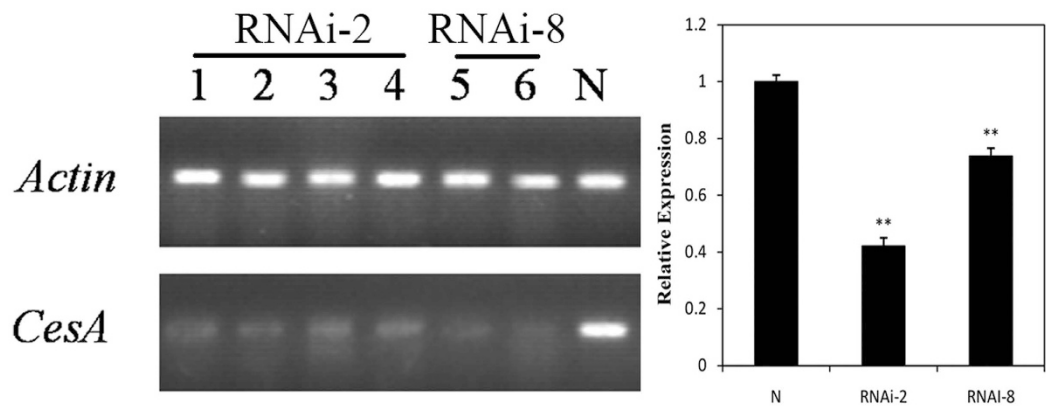


Figure 4. RT-PCR analysis of the T3 of RNAi plants and the control broccoli plants. *Actin*: Agarose gel of RT-PCR products amplified by the primers of *Actin*. *CesA*: Agarose gel of RT-PCR products amplified by the primers of *BoiCesA*. 1~4: these plants belonged to transgenic line 2 which had been chosen to measure the cellulose content 5~6: these plants belonged to transgenic line 8 which had been chosen to measure the cellulose content. N: The control plants.

Anatomic and ultrastructural changes. The difference of tissue structure between the T3 of RNAi plants and the control broccoli was surveyed by the light microscopy. The vascular bundles was reduced on the transverse sections located in the elongation zone of leaf veins. Compared with the control plant, the development of lateral veins was not observed in the T3 plant (Fig. 6). Meanwhile, all cells of the vascular bundles of the RNAi plants reduced expansion or elongation but the control plant had the normal leaf veins, compared to control plant, the content of vascular bundles of RNAi plants was approximately 56% (Fig. 6).

Scanning electron microscopy of the leaves from the control plants showed that the abaxial surface were generally smooth, and the epidermal cells were arrayed orderly (Fig. 7a). The stomata of the control plantlets displayed the normal morphology with kidney-shaped guard cells (Fig. 7c). On the contrary, there were many clumps of the epidermal cells along the abaxial surface, especially adjoin to leaf vein in RNAi plants (Fig. 7b). The RNAi and the control leaves also differed in the stomata morphological specificity, the T3 of RNAi leaves presented the abnormal stomata, with guard cells drastically deformed due to the swollen epidermal cells (Fig. 7d). The deformation of guard cells could possibly affect the stomatal function.

Moreover, some significant differences were also observed between the ultrastructure of chloroplasts in the T3 of RNAi and the control leaves. The results of transmission electron microscopy showed that the control cells chloroplasts of mesophyll cells contained the entire double membranes, the regular and inseparable layer of chloroplast grana and stroma, which overflow with starch grains (Fig. 7e). Whereas in the RNAi plants the layer of the slender and spindle-shaped chloroplast grana and stroma were irregular and even disaggregated, but most of all, there was a great difference between the numbers and types of starch grain from the RNAi and the control leaves, furthermore numerous osmiophilic globules appeared in the RNAi plants (Fig. 7f).

The T3 of RNAi plants have altered cellulose and pectin content. It showed the cellulose and pectin content of the two transgenic lines (RNAi-2 and RNAi-8) and the control plants (Fig. 8). The result showed about 40% decline in the cellulose content and about 19% reduction in the pectin content of the RNAi plants with that in the control plants. There were significant differences ($P < 0.05$) in cell wall materials between *CesA* T3 plants and control plants. It implied that the hairpin structure could affect cellulose biosynthesis.

Proline and soluble sugar contents in the RNAi plants. Accumulation of proline and soluble sugar is often related to plant adaptation to environmental stresses. Then in order to investigate the correlation of cellulose synthesis and plant physiological characters, proline and soluble sugar contents in T3 and control plants were measured under normal conditions. The two transgenic lines (RNAi-2, RNAi-8) respectively accumulated approximately 3 times higher proline contents than the control plants (Fig. 9a). At the same time, we found that the soluble sugar content of RNAi lines was higher ($P < 0.01$) than that in control plants (Fig. 9b).

RNAi plants has higher salt resistance capability. In normal conditions, compared with control plants, the T3 of RNAi plants were dwarf phenotype with smaller dark green leaves (Fig. 10a and b). Under 250 mM NaCl treatment, the leaves of T3 were still green with thick waxy on the surface (Fig. 10d) whereas the control plants became bleached (Fig. 10c). Moreover under the NaCl treatment, the dry weight of control plants significant reduced relative to that of RNAi plants (Fig. 10e).

Higher plants have developed an antioxidant defense system that includes the antioxidant enzymes SOD, POD, CAT, and APX to deal with adversity stress⁴⁴. The enzymatic activity analysis of antioxidant system was conducted in transgenic and control broccoli under the NaCl treatment (Fig. 11). After 3 weeks of NaCl treatment, the SOD activity of RNAi plants was about 3-fold higher than that of control plants (Fig. 11a). The activities of POD, CAT and APX of RNAi lines showed similar trends (Fig. 11b, c and d).

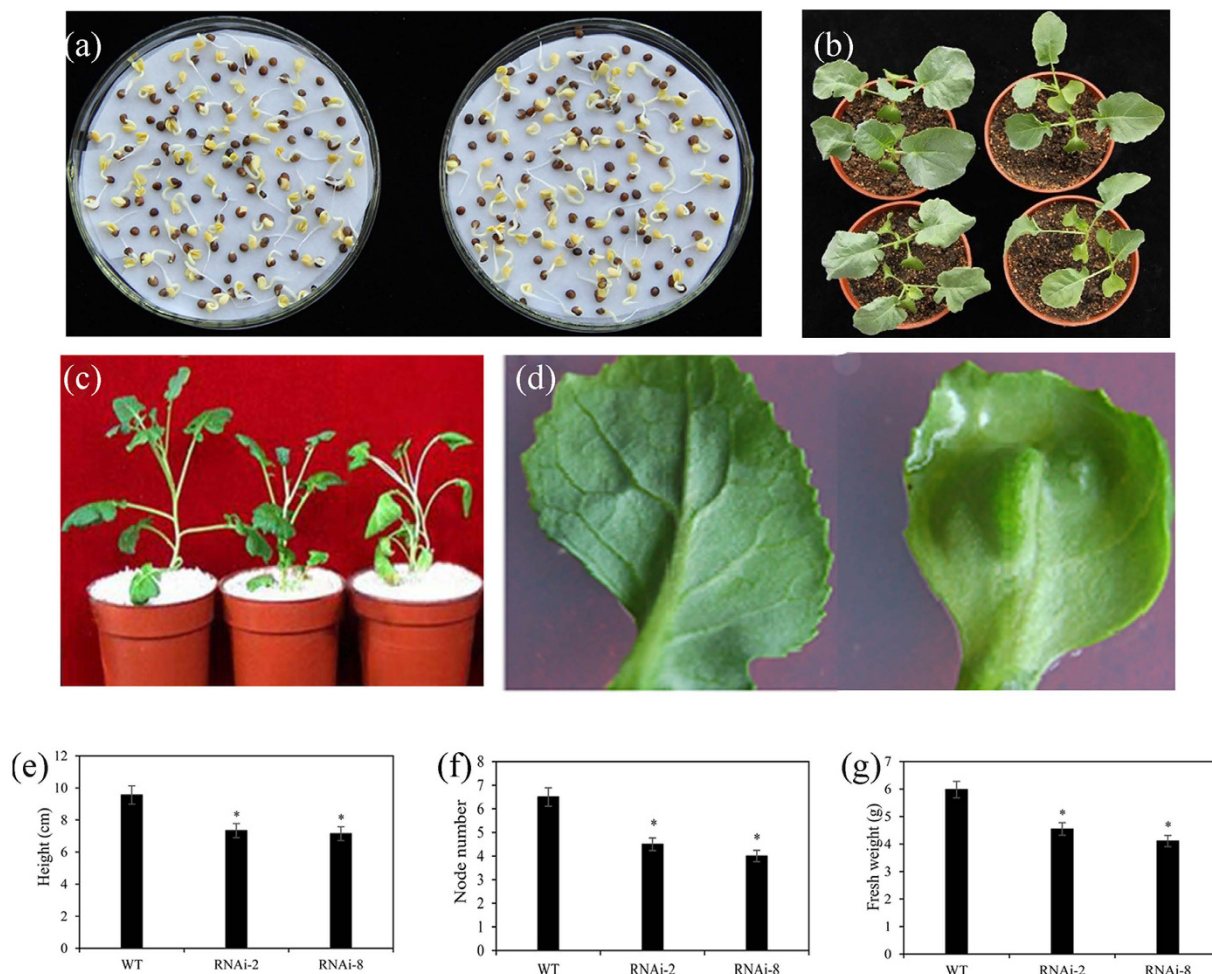


Figure 5. Analysis of phenotype of the broccoli plants. (a) The rate of germination between control (left) and transgenic plants (right). (b) Growth of control (left) and transgenic plants (right) with three weeks. (c) Show left to right is a pFGC1008 plant (control), two RNAi plants. The RNAi plants have obvious change in plant height. (d) The underside surface of the leaves are taken from the control plants (left), the RNAi plants (right). The lumps are evident and the texture is crunchy in RNAi plants compared with controls. (e) The measurement of height of control and transgenic plants. (f) Comparison of node number of control and transgenic plants. (g) Analysis of fresh weight for control and transgenic plants. (Values are mean \pm SE, $n = 3$, * $P < 0.05$, ** $P < 0.01$).

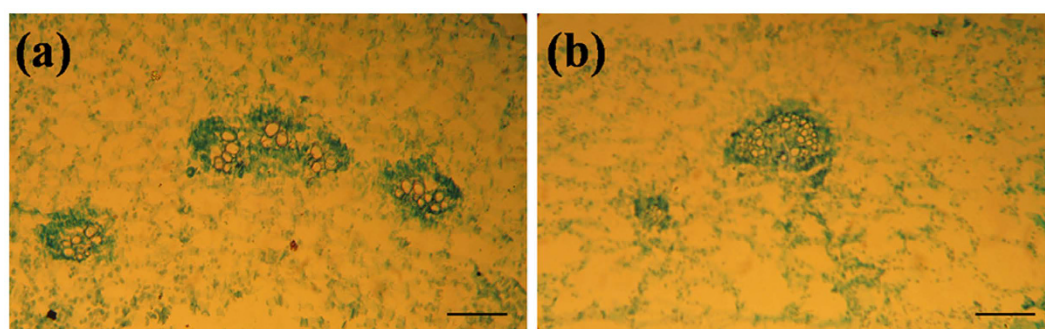


Figure 6. Light microscopic analysis of the control broccoli plants and the T3 of RNAi plants. (a) Transverse section of the leaf vein in control plants. (b) Transverse section of the leaf vein in the T3 of RNAi plants. All cells of the vascular bundles showed reduced expansion compared with the control plants. Bars indicate 100 μ m for (a,b).

BoiCesA affects the expression of genes related to salt tolerance. To further investigate the NaCl resistant mechanism of T3 of RNAi plants, we analyzed the expression of genes related to salt tolerance. Due to the lack of broccoli genome information, this brings some difficulties in our study. Based on the results of previous

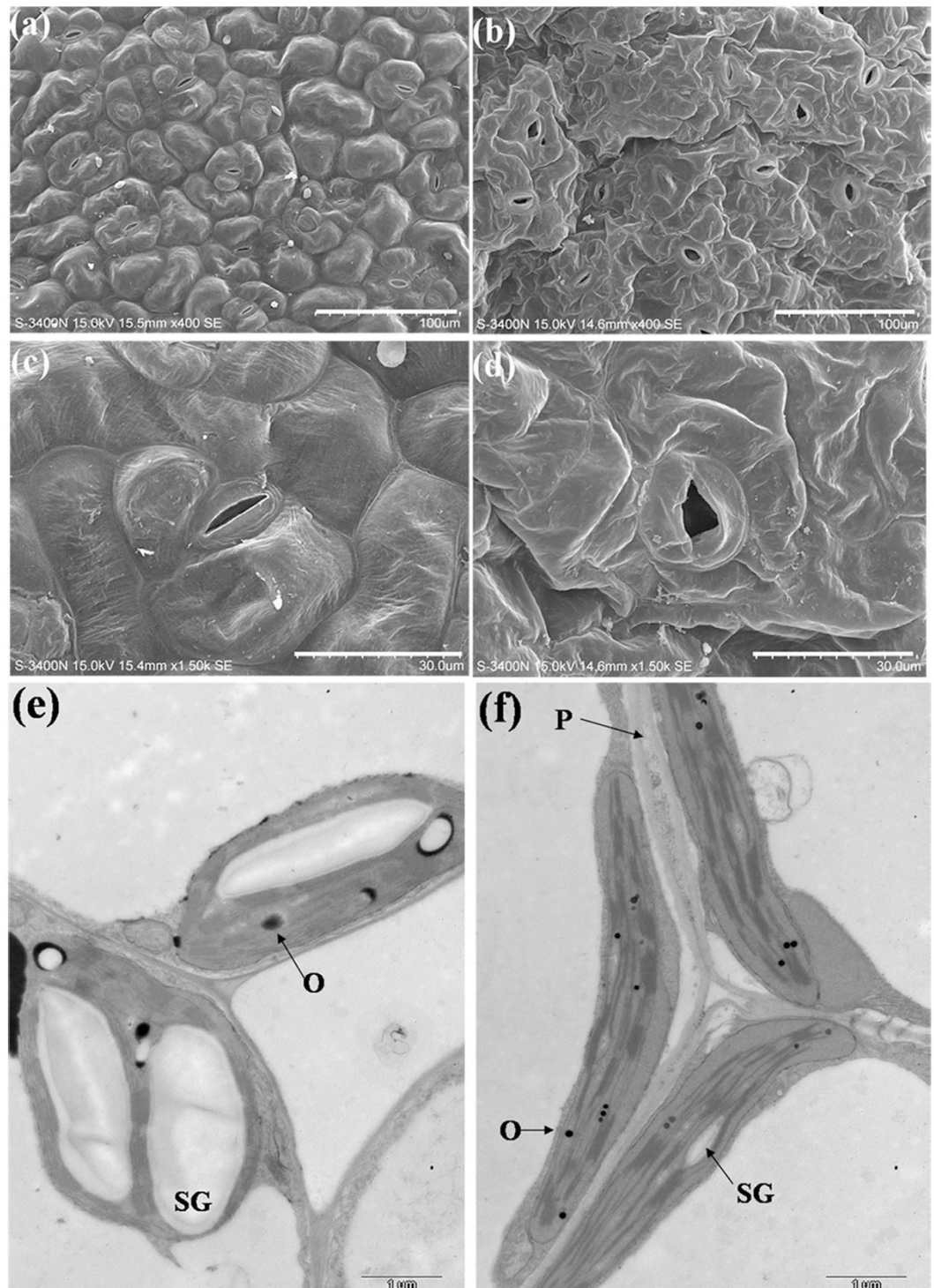


Figure 7. Scanning and transmission electron microscopic analysis of the control broccoli plants and the T3 of RNAi plants. (a) Abaxial surface of the control leaves showing smooth epidermal cells. Bar = 100 μ m. (b) Abaxial surface of the T3 of RNAi leaves showing swollen epidermal cells. Bar = 100 μ m. (c) Normal stomata of the control leaves with kidney-shaped guard cells. Bar = 30 μ m. (d) Abnormal stomata of the T3 of RNAi leaves with deformations of guard cells. Bar = 30 μ m. (e) Normal chloroplast of the control leaves with the regular and inseparable layer of chloroplast grana and stroma, which overflow with starch grains. Bar = 1 μ m. (f) Chloroplast of the T3 of RNAi leaves shows the numbers and types of starch grain differ from the control plants, numerous osmiophilic globules appear in the T3 plants. Bar = 1 μ m. O: osmiophilic globules; P: plasmolysis; SG: starch grain.

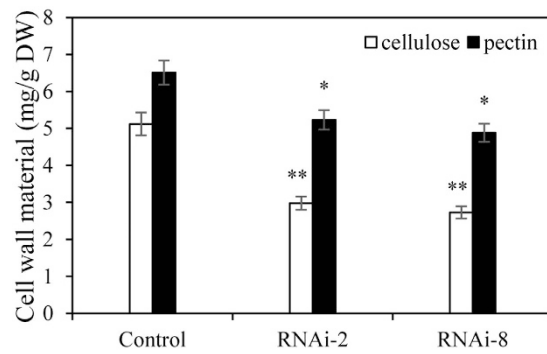


Figure 8. Comparison of cell wall composition of the control plants and transgenic plants. The content of cellulose and pectin in cell wall prepared from the control plants and transgenic plants (RNAi-2, RNAi-8). Results are significantly different from control under the same treatment conditions (Values are mean \pm SE, $n = 3$, * $P < 0.05$, ** $P < 0.01$).

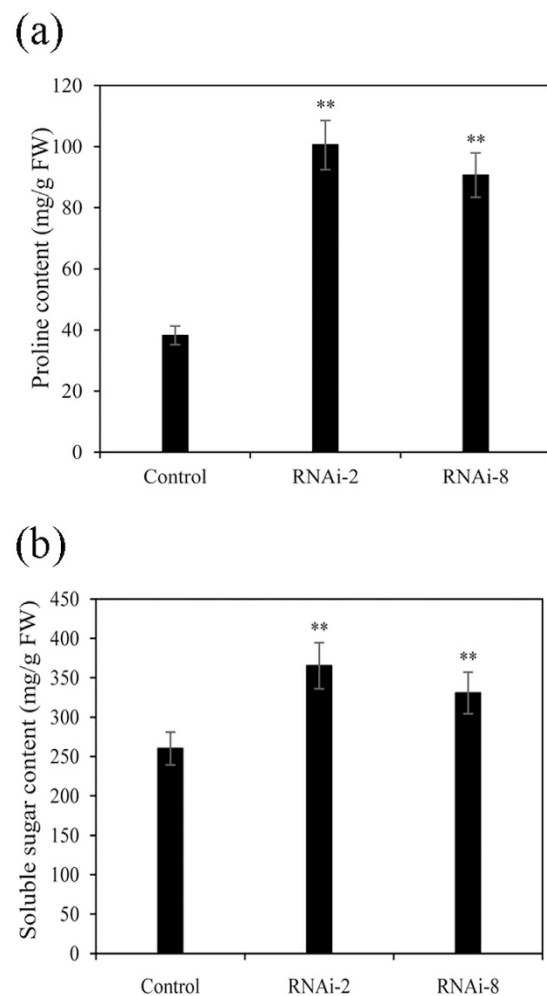


Figure 9. Content of proline (a) and soluble sugars (b) in RNAi and control plants under normal culture conditions. Values represent the mean \pm SE from three independent experiments.

studies^{45–47}, we found that *BoiProDH*, *BoiPIP2;2* and *BoiPIP;3* genes are associated with the salt tolerance of plants (Fig. 12). The expression level of *BoiProDH* was significantly reduced in T3 of RNAi plants, it was about 0.5 time that of WT, while the expressions level of *BoiPIP2;2* and *BoiPIP2;3* up-regulated in T3 of RNAi plants, it were 6–7 times than those of WT, these results might explain the altered salt tolerance of T3 of RNAi plants.

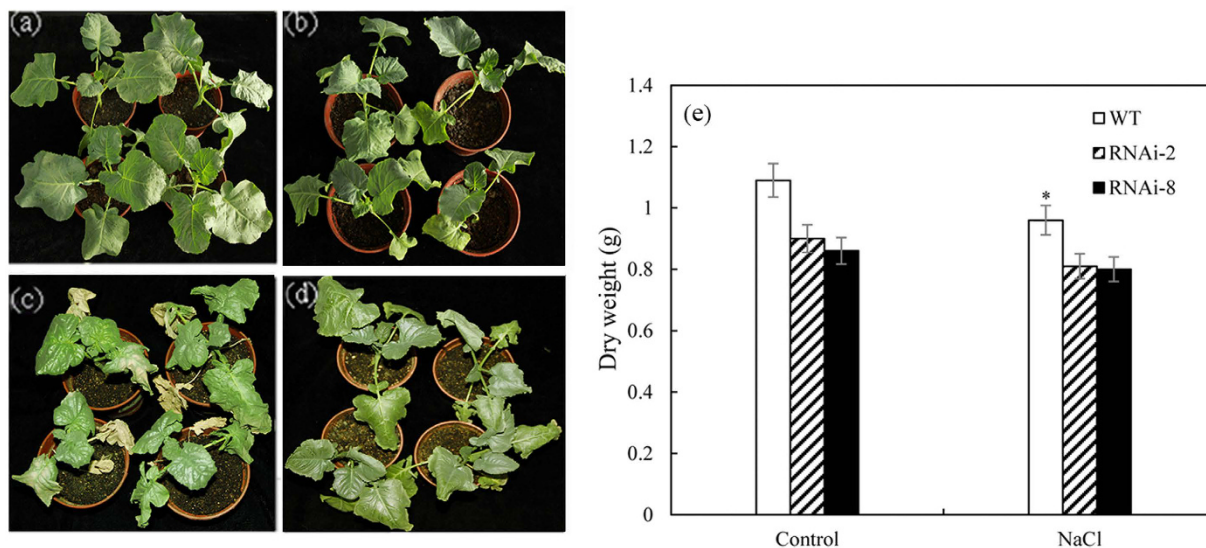


Figure 10. The RNAi plants are more NaCl tolerant than control plants. (a) Control plants without treatment. (b) The RNAi plants without treatment, RNAi-2 in left, RNAi-8 in right. (c) Control plants are bleached with 250 mM NaCl treatment for three weeks. (d) After 250 mM NaCl treatment for three weeks, there is no obvious change in RNAi transgenic plants. (e) Analysis of dry weight for control and transgenic plants under the NaCl treatment. Results are significantly different from control under the same treatment conditions (Values are mean \pm SE, $n = 3$, $*P < 0.05$, $**P < 0.01$).

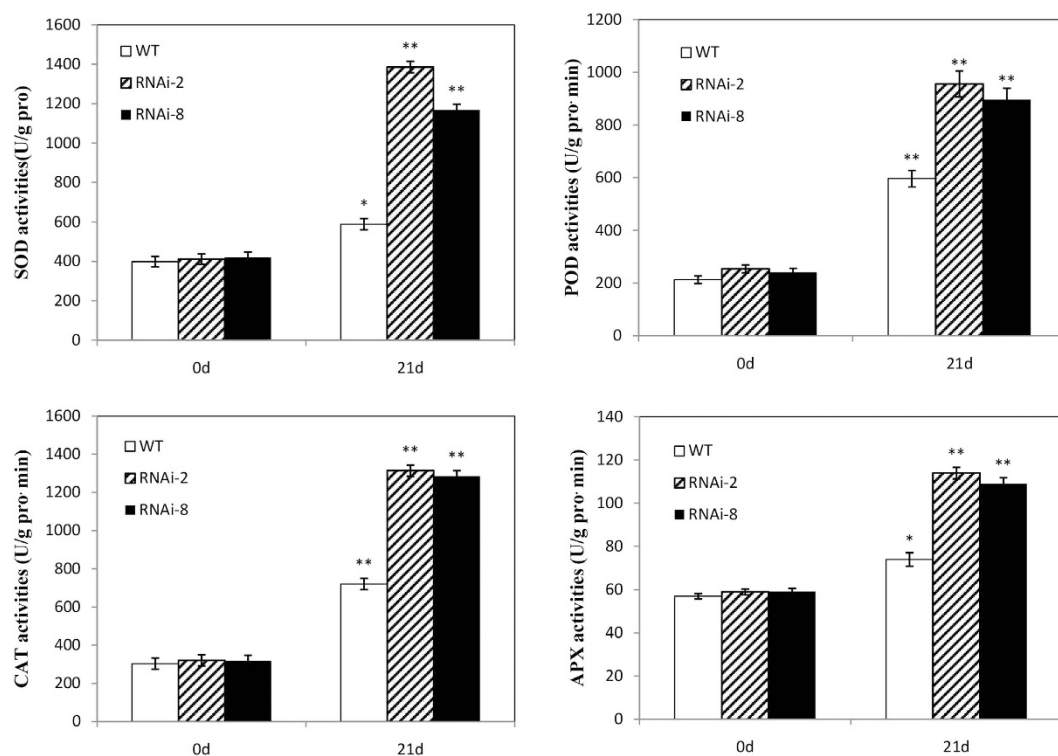


Figure 11. The measurement of superoxidisedismutase (SOD) (a), peroxidase (POD) (b), catalase (CAT) (c) and ascorbateperoxidase (APX) (d) activities in broccoli plants under Salt treatment. Values are mean \pm SE, $n = 3$, $*P < 0.05$, $**P < 0.01$.

Discussion

The function of the cDNA corresponding to putative cellulose synthase gene from *Brassica oleracea* L. was analyzed by RNAi. In our study, in attempt to verify the function of the given *BoiCesA* gene, we constructed the special RNAi vector using the specific region of *CesA* gene which could be the basis of the multiple alignments. Based

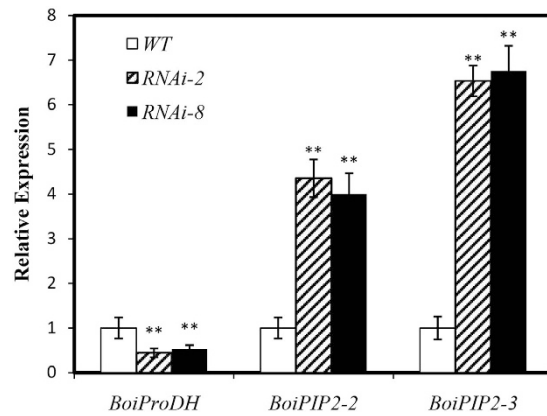


Figure 12. qRT-PCR of three genes differentially expressed in the WT and T3 of RNAi plants. Values are mean \pm SE, $n = 3$, * $P < 0.05$, ** $P < 0.01$.

on the alignments for *CesA* gene from rice previously described, the phylogenetic relationship resulting from the analysis whether based on the alignments from complete amino acid sequences or the hypervariable region (HVR) sequences was the same, and the sub-class identify was primarily defined by the HVR. The sequence in this region does not vary among members of the same sub-class, these experiments already considered that the region was termed 'class-specific region (CSR)'⁴⁸. Hence, we chose the cDNA fragment located in the HVR region to inhibit the specific *BoiCesA* gene exclusively (see domain structure for plant *CesA* in Fig. 1a). It could void the lethal phenotype if several endogenous *CesA* genes were silenced by interference of the homologous region of all *CesA* genes; this phenomenon had been indicated²².

On the other hand, examination of the leaves from the T3 of RNAi plants by light and electron microscopy indicated extensive reduction of cell expansion in vascular bundles, particularly on their abaxial surface, the wider stomatal aperture and the changes of chloroplast ultrastructure due to the down-regulation of *BoiCesA* gene.

Previous theory has confirmed that microtubules and actin filaments form highly organized arrays in stomatal cells that play key roles in the morphogenesis of stomatal complexes⁴⁹. Moreover, the cellulose fibrils and microtubules as well as actin filaments are radially distributed in guard cells⁵⁰. The depositing cellulose microfibril affects the pattern of local wall thickenings and the mechanical properties of the walls of stomatal cells, thus regulates accurately their shape⁴⁹. In our study, the modulation of cellulose content caused by the RNAi-induced silencing of the specific *BoiCesA* gene might be the reason of the wider stomatal aperture compared with the control, or, the reduction of the depositing cellulose micro-fibrils weakened support to the guard cells' shape. In addition, we also observed the degradation of starch and the appearance of numerous osmiophilic globules in chloroplasts. The ultrastructural changes of leaves have been reported in wheat and corn⁵¹. The chloroplasts in sugarcane cultivar YT57/423 were collapsed, presenting many osmiophilic granules⁵². In addition under drought stress conditions, the chloroplasts' lengths decreased and their widths increased, rendering them round in shape. Drought stress also significantly changed the internal structure of the chloroplasts. Membrane systems were damaged, starch grains disappeared, the chloroplasts became deformed and vacuolized⁵³. Therefore, under stress condition, in chloroplasts the rapid degradation of starch and soluble sugars accumulation were occurred. Previous studies showed that drought stress can improve the content of some sugars, which may be suppressed some enzyme activities related to cellulose synthesis⁵⁴, the *leaf wilting2* mutants which are new alleles of the *AtCesA8/IRX1* gene revealed that cellulose synthesis is important for stress responses containing drought induction of gene expression⁵⁵. Our results suggest that regulation cell wall cellulose synthesis are significant influencing factors in polysaccharide metabolism and adaptations of plants to salt stress.

We know that the proline and soluble sugar are important osmotic protective substance that involved in osmotic adjustment⁵⁶. It reported that proline acted as a compatible solute in the cytoplasm. The accumulation of proline can stabilize the macromolecules^{57,58}. A central role of soluble sugars depends not only on their direct involvement in the synthesis of other compounds and energy provision, but also on stabilization of membranes⁵⁹. The increment of soluble sugar and proline content associated with reductions in cellulose confirmed that the cell wall could not only perceive, but also adjust for physical changes in its structure.

Under the biotic and abiotic stress, the reduction of cellulose content was observed⁶⁰. In the experiment the cellulose synthesis is important for NaCl stresses response. Compared with control plants, the T3 of RNAi plants were more tolerant to NaCl treatment. Cellulose is the main load-bearing component of cell wall. The change of cellulose content often generates obvious consequences either compensatory or integrity responses. For example, plants may be made more tolerant to stresses as drought, salt and osmotic stress by mutations at *AtCESA8* gene which encodes a subunit of a cellulose synthesis complex⁵⁵. The *eli1* mutants of *CESA3* in *Arabidopsis thaliana* cause reduced cellulose synthesis, activating defense response through jasmonate and ethylene signaling pathways⁶¹. Those researches indicate that this is probably a general consequence of *CESA* loss-of- function.

In this study, we found the obvious starch degradation and soluble sugar accumulation in RNAi plants. It is possible that starch could be converted into soluble sugar, which might resulted in the increase of soluble sugar content, and enhanced the salt tolerance ability of plants. On the other hand, knockdown of a cellulose synthase gene *BoiCesA* inhibited the synthesis of cellulose, might lead to the substrate of cellulose synthesis into

other metabolic pathways, resulted increased soluble sugar content, which is involved in the intracellular osmotic potential. These inferences are still pending for further experimental verification.

Proline accumulation is a common response to osmotic stress in many plants. Proline dehydrogenase (ProDH) is a key enzyme that catalyzes the degradation of proline in the mitochondria⁴⁵. Our previous results proved that it was effective to increase the accumulation of free proline by silencing *BoiProDH* gene under salt stress⁴⁶. We found that the *BoiProDH* expression in RNAi plants was significantly decreased, which might reveal the proline accumulation in RNAi plants.

Aquaporins (AQPs), which play a regulatory role in cellular water transport also called membrane protein family MIP (major intrinsic protein). The function of aquaporin protein abundant, such as water transport, osmotic adjustment, abiotic stress response. Our previous study confirmed that SIPIPs through improving plant water content and maintaining osmotic balance to improve the ability of tomato drought resistance⁶². *BoiPIP2s* plays important roles in the response of broccoli to salinity⁴⁷. The expressions of *BoiPIP2;2* and *BoiPIP2;3* in T3 of RNAi plants were significantly higher than in WT plants, this suggested that the excessive expression of genes related to salt tolerance enhanced the salt tolerance of RNAi plants.

Cellulose content has an influence on the vegetable quality and resistance. *BoiCesA* may play a crucial role in the control of cellulose biosynthesis, and it is the first report of the *CesA* gene cloned from broccoli, according to the genetic relationship of *CesA* genes in different plants. Based on the different plant *CesA* genes dendrogram, we predict that the *BoiCesA* clone is a member of *CesA* family and the *BoiCesA* clone may share functional similarity with the *Arabidopsis* genes in the same cluster. Without the function of the *CesA1*, *CesA2*, *CesA3* and *CesA6* genes, the cellulose of primary wall are difficultly biosynthesized from mutants^{17,23,63,18}. So we suggest that the *BoiCesA* clone may play a role in primary cell wall biosynthesis.

References

- Ferguson, L. R., Robertson, A. M. & McKenzie, R. I. Adsorption of a hydrophobic mutagen to dietary fiber from taro (*Colocasia esculenta*), an important food plant of the South Pacific. *Nutrition and Cancer* **171**, 85–95 (1992).
- Haiger, C. H. *et al.* Carbon partitioning to cellulose synthesis. *Plant Molecular Biology* **47**, 29–51 (2001).
- Doblin, M. S., Kurek, I., Jacob-Wilk, D. & Delmer, D. P. Cellulose biosynthesis in plants: from genes to rosettes. *Plant Cell Physiology* **43**, 1407–1420 (2002).
- Pear, J. R., Kawagoe, Y., Schreckengost, W. E., Delmer, D. P. & Stalker, D. M. Higher plants contain homologs of the bacterial *celA* genes encoding the catalytic subunit of cellulose synthase. *Proceeding of the National Academy Science USA* **93**, 12637–12642 (1996).
- Delmer, D. P. Cellulose biosynthesis: exciting times for a difficult field of study. *Annual of Review of Plant Physiology and Plant Molecular Biology* **50**, 245–276 (1999).
- Richmond, T. Higher plant cellulose synthases. *Genome Biology* **1**, 3001 (2000).
- Cutler, S. & Somerville, C. Cloning in silico. *Current Biology* **7**, R108–R111 (1997).
- Richmond, T. A. & Somerville, R. C. The cellulose synthase superfamily. *Plant Physiology* **124**, 495–498 (2000).
- Hamann, T. *et al.* Global expression analysis of *CESA* and *CSL* genes in *Arabidopsis*. *Cellulose* **11**, 279–286 (2004).
- Djerbi, S. *et al.* Identification and expression analysis of genes encoding putative cellulose synthases (*CesA*) in the hybrid aspen, *Populustrēmula* (L.) × *P. tremuloides* (Michx.). *Cellulose* **11**, 301–312 (2004).
- Saxena, I. M. & Brown, R. M. Identification of a second cellulose synthase gene (*acsAII*) in *Acetobacter xylinum*. *Journal of Bacteriology* **177**, 5276–5283 (1995).
- Saxena, I. M. & Brown, R. M. Jr. Identification of cellulose synthase(s) in higher plants. *Cellulose* **4**, 33–49 (1997).
- Campbell, J. A., Davies, G. J., Bulone, V. V. & Henrissat, B. A classification of nucleotide-diphospho-sugar glycosyltransferases based on amino acid sequence similarities. *Journal of Biochemistry* **326**, 929–939 (1997).
- Charnock, S. J. & Davies, G. J. Structure of the nucleotide-diphospho-sugar transferase, *SpsA* from *Bacillus subtilis*, in native and nucleotide-complex forms. *Biochemistry* **38**, 6380–6385 (1999).
- Charnock, S. J., Henrissat, B. & Davies, G. J. Three dimensional structures of UDP-sugar glycosyltransferases illuminate the biosynthesis of plant polysaccharides. *Plant Physiology* **125**, 527–531 (2001).
- Kurek, I., Kawagoe, Y., Jacob-Wilk, D., Doblin, M. & Delmer, D. Dimerization of cotton fiber cellulose synthase catalytic subunits occurs via oxidation of the zinc-binding domains. *Proceeding of the National Academy Science USA* **99**, 11109–11114 (2002).
- Arioli, T. *et al.* Molecular analysis of cellulose biosynthesis in *Arabidopsis*. *Science* **279**, 717–720 (1998).
- Fagard, M. *et al.* PROCUSTE1 encodes a cellulose synthase required for normal cell elongation specifically in roots and dark-grown hypocotyls of *Arabidopsis*. *Plant Cell* **12**, 2409–2423 (2000).
- Turner, S. R. & Somerville, C. R. Collapsed xylem phenotype of *Arabidopsis* identifies mutants deficient in cellulose deposition in the secondary cell wall. *Plant Cell* **9**, 689–701 (1997).
- Taylor, N. G., Scheible, W. R., Cutler, S., Somerville, C. R. & Turner, S. R. The irregular xylem3 locus of *Arabidopsis* encodes a cellulose synthase required for secondary cell wall synthesis. *Plant Cell* **11**, 769–779 (1999).
- Turner, S., Taylor, N. & Jones, L. Mutations of the secondary wall. *Plant Molecular Biology* **47**, 209–219 (2001).
- Burn, J., Hocart, C. H., Birch, R., Cork, A. C. & Williamson, R. E. Functional analysis of the cellulose synthase genes *CesA1*, *CesA2*, and *CesA3* in *Arabidopsis*. *Plant Physiology* **129**, 797–807 (2002).
- Oomen, R. J. F. J., Tzitzikas, E. N., Bakx, E. J., Straatman-Engelen, I. & Bush, M. S. Modulation of the cellulose content of tuber cell wall by antisense expression of different potato (*Solanum tuberosum* L.) *CesA* clones. *Phytochemistry* **65**, 535–546 (2004).
- Saxena, I. M., Brown, R. M. Jr., Fevre, M., Geremia, R. A. & Henrissat, B. Multidomain architecture of beta-glycosyltransferases, implications for mechanism of action. *Journal of Bacteriology* **177**, 1419–1424 (1995).
- Burton, R. A. *et al.* Virus-induced silencing of a plant cellulose synthase gene. *Plant Cell* **12**, 691–705 (2000).
- Holsters, M. *et al.* *In vivo* transfer of the ti-plasmid of *Agrobacterium tumefaciens* to *Escherichia coli*. *Molecular and General Genetics* **163**(3), 335338 (1978).
- Qin, Y., Li, H. L. & Guo, Y. D. High-frequency embryogenesis, regeneration of broccoli (*Brassica oleracea* var. *italica*) and analysis of genetic stability by RAPD. *Scientia Horticulturae* **111**, 203–208 (2007).
- Wang, Z. *et al.* A Practical Vector for Efficient Knockdown of Gene Expression in Rice (*Oryza sativa* L.). *Plant molecular Biology Reporter* **22**, 409–417 (2004).
- Johanson, D. A. *Plant Microtechnique*. McGraw Hill Co, New York (1940).
- Yu, Y., Zhao, Y. Q., Zhao, B., Ren, S. X. & Guo, Y. D. Influencing factors and structural characterization of hyperhydricity of *in vitro* regeneration in *Brassica oleracea* var. *italica*. *Canadian Journal of Plant Science* **91**(1), 159–165 (2011).
- Kutík, J., Kočová, M., Holá, D. & Körnerová, M. The development of chloroplast ultrastructure and Hill reaction activity during leaf ontogeny in different maize (*Zea mays* L.) genotypes. *Photosynthetica* **36**, 497–507 (1999).

32. Zablackis, E., Huang, J., Muller, B., Darvill, A. G. & Albersheim, P. Characterization of the cell-wall polysaccharides of *Arabidopsis thaliana* leaves. *Plant Physiology* **107**, 1129–1138 (1995).
33. Zhou, H. L. *et al.* OsGLU1, a putative membrane-bound endo-1, 4- β -D-glucanase from rice, affects plant internode elongation. *Plant Molecular Biology* **60**, 137–151 (2006).
34. Selvendran, R. R. & O'Neill, M. A. Isolation and analysis of cell walls from plant material. *Methods of Biochemical Analysis* **32**, 25–153 (1987).
35. Yu, L. R. & Love, C. A. Strawberry texture and pectin content as affected by electron beam irradiation. *Journal of Food Science* **61**, 844–848 (1996).
36. Wang, Y. C., Chuang, Y. C. & Hsu, H. W. The flavonoid, carotenoid and pectin content in peels of citrus cultivated in Taiwan. *Food Chemistry* **106**, 277–284 (2008).
37. Troll, W. & Lindsley, J. A photometric method for the determination of proline. *Journal of Biological Chemistry* **215**, 655–660 (1955).
38. Dubois, M., Gilles, K. A., Hamilton, J. K., Rebers, P. A. & Smith, F. Colorimetric method for determination of sugars and related substances. *Analytical Chemistry* **28**, 350–356 (1956).
39. Giannopolitis, C. N. & Ries, S. K. Superoxide dismutases. 1. occurrence in higher-plants. *Plant Physiology*, **59**, 309–314 (1977).
40. Scebba, F., Sebastiani, L. & Vitagliano, C. Activities of antioxidant enzymes during senescence of *Prunus armeniaca* leaves. *Biological Plant* **44**, 41–46 (2011).
41. Kato, M. & Shimizu, S. Chlorophyll metabolism in higher plants. 7. chlorophyll degradation in senescing tobacco-leaves-phenolic-dependent peroxidative degradation. *Canadian journal of botany-revue canadienne de botanique* **65**, 729–735 (1987).
42. Nakano, Y. & Asada, K. Hydrogen-peroxide is scavenged by ascorbate-specific peroxidase in spinach-chloroplasts. *Plant Cell Physiology* **22**, 867–880 (1981).
43. Griffiths, P. D. & Tonguc, M. Genetic relationships of Brassica vegetables determined using database derived simple sequence repeats. *Euphytica* **37**, 193–201 (2004).
44. Galano, A., Tan, D. X. & Reiter, R. J. Melatonin as a natural ally against oxidative stress: a physicochemical examination. *Journal of Pineal Research* **51**, 1–16 (2011).
45. Wang, H., Tang, X., Wang, H. & Shao, H. Proline Accumulation and Metabolism-Related Genes Expression Profiles in *Kosteletzkya virginica* Seedlings Under Salt Stress. *Front Plant Sci.* **6** (2015).
46. Yang, P. *et al.* Cloning and Functional Identification of ProDH Gene from Broccoli. *Genomics and Applied Biology* **29**, 206–214 (2010).
47. Muries, B., Faize, M., Carvajal, M. & Del Carmen Martinez-Ballesta, M. Identification and Differential Induction of the Expression of Aquaporins by Salinity in Broccoli Plants. *MolBiosyst.* **7**, 1322–1335 (2011).
48. Vergara, C. E. & Carpita, N. C. β -D-Glycan synthases and the *CesA* gene family: lessons to be learned from the mixed-linkage (1 \rightarrow 3), (1 \rightarrow 4) β -D-glucan synthase. *Plant Molecular Biology* **47**, 145–160 (2001).
49. Galatis, B. & Apostolakis, P. The role of the cytoskeleton in the morphogenesis and function of stomatal complexes. *New Phytologist* **161**, 613–639 (2004).
50. Raschke, K. Movement of stomata in plant. *Physiology of Movements* **7**, 382–441 (1979).
51. Jian, L. C. & Wang, H. *Stress plant cell biology* (Beijing: Science Press, 159–167 (2009).
52. Zhong, X. Q. & Ye, Z. B. Changes of the ultrastructure in sugarcane leaves after the drought. *Journal of South China Agricultural University* **13**(3), 64–68 (1992).
53. Meng, J. F., Xu, T. F. & Wang, Z. Z. The ameliorative effects of exogenous melatonin on grape cuttings under water-deficient stress: antioxidant metabolites, leaf anatomy, and chloroplast morphology. *Journal of Pineal Research* **57**, 200–212 (2014).
54. Foyer, C. H., Valadier, M. H., Migge, A. & Becker, T. W. Drought-induced effects on nitrate reductase activity and mRNA and on the coordination of nitrogen and carbon metabolism in maize leaves. *Plant Physiology* **117**, 283–292 (1998).
55. Chen, Z. Z. *et al.* Disruption of the cellulose synthase gene, *AtCesA8/IRX1*, enhances drought and osmotic stress tolerance in *Arabidopsis*. *The Plant Journal* **43**, 273–283 (2005).
56. Yancey, P. H., Clark, M. E., Hand, S. C., Bowlus, R. D. & Somero, G. N. Living with water stress: Evolution of osmolyte system. *Science* **217**, 1214–1222 (1982).
57. Samaras, Y. *et al.* Proline accumulation during water deficit in: Smirnoff, N. (Ed.) *Environment and plant metabolism*. (Flexibility and acclimation, Bios Scientific Publ., Oxford, UK, pp. 161–187 (1995).
58. Smirnoff, N. & Stewart, G. R. Stress metabolites and their role in coastal plants. *Vegetatio* **62**, 273–278 (1985).
59. Hoekstra, F. A., Golovina, E. A. & Buitink, J. Mechanisms of plant desiccation tolerance. *Trends Plant Sci.* **6**, 431–438 (2001).
60. Humphrey, T. V., Bonetta, D. T. & Goring, D. R. Sentinels at the wall: cell wall receptors and sensors. *New Phytologist* **176**, 7–21 (2007).
61. Ellis, C. *et al.* The *Arabidopsis* mutant *cev1* links cell wall signalling to jasmonate and ethylene responses. *Plant Cell* **14**, 1557–1566 (2002).
62. Li, R. *et al.* Plasma Membrane Intrinsic Proteins S1PIP2;1, S1PIP2;7 and S1PIP2;5 Conferring Enhanced Drought Stress Tolerance in Tomato. *Sci Rep-UK.* **6** (2016).
63. Desprez, T. *et al.* Resistance against herbicide isoxaben and cellulose deficiency caused by distinct mutations in same cellulose synthase isoform CESA6. *Plant Physiology* **128**, 482–490 (2002).

Acknowledgements

We thank Prof. Zhizhong Gong (China Agricultural University) for helpful discussions and suggestions. This work was partly supported by the grants to Guo (2016YFD0101000 from Ministry of Science and Technology of China, BLVT-03 from Beijing Agriculture Bureau), to Ma (2016ZX08004-002-009 from the Ministry of Agriculture of China) and by Beijing Key Laboratory of Growth and Developmental Regulation for Protected Vegetable Crops.

Author Contributions

Yang-Dong Guo and Ying Wang designed research; Ying Wang, Shuangtao Li, Fengfeng Xu, Lei Zhang, Mengyun Liu and Yang-Dong Guo performed research; Ying Wang, Shuangtao Li, Fengfeng Xu, Peng Lin and Yang-Dong Guo analyzed data; Ying Wang, Yang-Dong Guo, Shuxin Ren and Rui Ma wrote the paper.

Additional Information

Supplementary information accompanies this paper at <http://www.nature.com/srep>

Competing financial interests: The authors declare no competing financial interests.

How to cite this article: Li, S. *et al.* Knockdown of a cellulose synthase gene *BoiCesA* affects the leaf anatomy, cellulose content and salt tolerance in broccoli. *Sci. Rep.* **7**, 41397; doi: 10.1038/srep41397 (2017).

Publisher's note: Springer Nature remains neutral with regard to jurisdictional claims in published maps and institutional affiliations.



This work is licensed under a Creative Commons Attribution 4.0 International License. The images or other third party material in this article are included in the article's Creative Commons license, unless indicated otherwise in the credit line; if the material is not included under the Creative Commons license, users will need to obtain permission from the license holder to reproduce the material. To view a copy of this license, visit <http://creativecommons.org/licenses/by/4.0/>

© The Author(s) 2017